RSC Advances

PAPER

View Article Online
View Journal | View Issue

Cite this: *RSC Adv.*, 2022, **12**, 4681

Targeted delivery of capecitabine to colon cancer cells using nano polymeric micelles based on beta cyclodextrin

Hossein Ameli and Nina Alizadeh *

Nano polymeric micelles (nano PMs) help to increase accessibility to tumor sites, decrease side effects and allow controlled drug dissemination over a long period of time. The aim of this study was to optimize the delivery of the anticancer drug capecitabine (CAP) using nano PMs and cyclodextrin (CD) to allow the treatment of colon cancer. A pH-responsive copolymer was prepared and the variables of loading time, loading temperature, the amount of copolymer and also the ratio of acrylic/maleic copolymer to beta CD and the effect that these variables have on drug loading were investigated, with variable optimization studies carried out following a definitive screening design (DSD). The morphology and structure of the particles were determined by scanning electron microscopy (SEM) and Fourier-transform infrared (FTIR) spectroscopy. *In vitro* drug release exemplified that the micelles were pH-sensitive, this action was shown that firstly the drug release was done perfectly targeted and under control and secondly the drug has been released above 80% inside the colon.

Received 21st October 2021
Accepted 17th January 2022

DOI: 10.1039/d1ra07791k

rsc.li/rsc-advances

1. Introduction

The trend in the pharmaceutical industry is to generate sustained-release formulations for drugs that require multiple daily doses to improve patient compliance and avoid the peaks and troughs in the drug plasma concentration often observed with the frequent dosing of immediate-release formulations. Recently, there has been interest in designing colon-specific drug delivery systems for the treatment of colon cancer, irritable bowel syndrome, inflammatory bowel disease (IBD) and infectious diseases.[1–4] Oral administration of drugs in the form of a colon-specific delivery system would increase drug bioavailability at the target site, reducing drug dose and systemic adverse effects. However, conventional oral dosage forms are ineffective in delivering drugs to the colon due to their absorption or degradation in the upper gastrointestinal tract.[5–8] Capecitabine (CAP), an oral prodrug of 5-fluorouracil (5-FU), is widely used in colorectal cancer,[9–13] and once it reaches the systemic circulation shows rapid absorption and converts into its active metabolite 5-FU *via* a tri-enzymatic step reaction.[14] Due to a short elimination half-life of 0.5–1 h and prescribed twice-daily dosing of 2.5 g m^{-2}, CAP causes severe adverse effects (cardiotoxicity, bone marrow depression, diarrhoea, nausea, vomiting, *etc.*) and creates an undesirable drug plasma concentration in the body.[15,16] Taking these issues as a major concern, there is a need to fabricate a controlled delivery system of CAP to maintain a therapeutic plasma drug concentration for an extended period. Thus, a reduction in adverse effects with improved patient compliance can be achieved. However, particle growth, unpredictable gelation tendency, burst release and drug expulsion after the polymeric transition process limits the practical usefulness of capecitabine (CAP). Hence, there is a need for an alternative drug delivery system for CAP to improve its therapeutic efficacy. Cyclodextrins (CDs) are naturally available water-soluble cyclic oligosaccharide-1,4-linked-glucopyranoses composed of six or more glucose units.[17] Due to their unique structural, physical and chemical properties, cyclodextrins and their derivatives have been of great interest for use in various fields, such as medicine, drug, agriculture, the cosmetics industry, and analytical chemistry. In particular, in the last few decades, the applications of cyclodextrins and their derivatives in the pharmaceutical industry have attracted research interest. Cyclodextrins are well known for their ability to increase solubility, dissolution rate and bioavailability of loaded drugs.[18] They have a ring structure with a hydrophilic outer surface and lipophilic cavity, which give them the ability to form non-covalent inclusion complexes with drug molecules of an appropriate size. Inclusion complexes have been very well explored to improve the water solubility and chemical stability of drugs.[19] The vast microbiota present in the colon, especially Bacteroides, break CDs into small saccharides *via* fermentation,[20–22] thus leading to rapid drug release. Moreover, the formation of short-chain fatty acids *via* the fermentation of CDs provides benefits to the maintenance of the health and integrity of the colonic epithelium.[23] These properties render CDs useful colon-targeting carriers. A combination of nano polymeric micelles (nano PMs) and β-CD can improve the drug loading

Department of Chemistry, Faculty of Science, University of Guilan, P.B. 41335-1914, Rasht, Iran. E-mail: n-alizadeh@guilan.ac.ir

capacity and therapeutic efficacy of drugs with poor water solubility. Recently, nano polymeric PMs have drawn major attention in drug delivery due to their properties, such as small particle size, good thermodynamic stability, increase in the solubility of hydrophobic drugs, prolonged drug release, and avoiding recognition by the reticuloendothelial system (RES). Nano PMs comprise a drug-loading core and a hydrophilic shell. An amphiphilic block copolymer forms micelles when in contact with an aqueous vehicle *via* self-assembly, resulting in hydrophobic interactions wherein hydrophobic drugs can be encapsulated into the central core of micelles through hydrophobic interactions.[24–26] These novel carriers have been successfully investigated for the delivery of various anticancer drugs, such as paclitaxel,[27–29] doxorubicin,[30,31] methotrexate,[32,33] *etc.*, to improve their therapeutic efficacy. Polymeric micelles are a class of colloidal dispersions, generally formed from amphiphilic block copolymers at or above their critical micelle concentration (CMC). These copolymers are composed of two distinct hydrophobic and hydrophilic domains. Due to the local phase separation of these hydrophobic and hydrophilic segments in aqueous solution, the copolymers can self-assemble into the spherical core–shell structure of the PMs. During micellization, the hydrophobic blocks of the copolymers self-associate into the micelle centre, away from the aqueous surroundings, to decrease the free energy of the system. However, the hydrophobic blocks locate between the core and external environment to form a shell (or corona). The presence of this hydrophilic corona makes the micelles stable and stealthy, helping them to avoid the RES, also allowing their prolonged circulation and residence time in the bloodstream. These advantages, together with their small size (100 nm), make PMs promising carriers for the administration of various insoluble and poorly soluble pharmaceutics that can be incorporated into the hydrophobic core of the micelles.[34–37] Another advantage of PMs is their ability to form various types of pH-responsive drug delivery systems depending on the encapsulated drug and physiological destination. The incorporation of pH-sensitive groups into the core-forming blocks makes PMs sensitive to environmental pH. In the most common strategy, ionization of the pH-sensitive groups of the inner blocks converts the micelle core from hydrophobic to hydrophilic, resulting in the demicellization of the copolymers and rapid release of the encapsulated hydrophobic drug. PMs containing acidic groups in their inner core can be used to design smart oral drug delivery systems.[38–42] Such assemblies are stable at the acidic pH of the stomach because their inner blocks are in their unionized and hydrophobic form. Upon a pH increase in the intestine, the acidic groups start deprotonation, which increases the electrostatic charge and hydrophilicity of the inner part, leading to micelle dissociation and drug release. Under certain pH conditions the functional groups presented along the backbone and side chains of the polymer undergo ionization that leads to a conformational change in the polymer resulting in its swelling or dissolution. pH-sensitive polymers are thus a class of polyelectrolytes with ionic functional groups that are weakly acidic (*e.g.*, carboxylic and sulfonic acids) or basic (*e.g.*, amines, imidazole, and pyridine).[43–47]

Acrylic/maleic copolymer is a copolymer of maleic anhydride and acrylic acid, which does not degrade below pH 7. The coating of pH-sensitive polymers to the tablets, capsules or pellets provide delayed release and protect the active drug from gastric fluid. A combination of nano PMs and β-CD can improve the drug loading capacity and therapeutic efficacy of poorly water soluble drugs. Nano PMs with CD is a pH-independent nanocomposite that contributes toward the delivery of drugs in the colon. In the analysis of problems affected by several factors with possible interactions, statistical screening methods are often adopted to select the parameters that actually affect the response variable and to eliminate irrelevant ones. This is particularly useful at the beginning of an investigation when little or no information is available for the system of interest. Recently, a new class of three-level designs, so-called definitive screening designs (DSD), has been proposed by Jones and Nachtsheim.[48] DSD allows the assessment of active effects, two-factor interactions and pure-quadratic effects in the presence of effector sparsity. This allows a dramatic reduction in the number of experiments, thus enabling significant savings in time and cost of materials. The definitive screening design enables the evaluation of several interdependent factors to define critical parameters that affect drug entrapment efficiency. The use of these screening methods has increased in recent years.[49–51] In the present study, we establish a drug delivery system using cyclodextrin and copolymer based on a pH responsive micelle mechanism for CAP drug delivery and release in colon cancer.

2. Materials and methods

2.1. Materials

β-CD (purity, >98%) was purchased from Sigma. The drug capecitabine (purity, >99%) was obtained from the Aria Pharmaceutical Company. Acrylic/maleic copolymer (purity, >92%) with a molar mass of 70 000 g mol^{-1} and brand CP 5 powder were purchased from BASF Germany. Dialysis membrane (MWCO 12 kDa) was purchased from Sigma. All other reagents and chemicals were of analytical grade and purchased from Sigma.

2.2. Characterization

UV-vis absorption measurements were carried out at room temperature using a UV 1800 spectrophotometer (SHIMADZU, Japan). The UV-vis spectra of the samples were recorded in the frequency range of 200–700 nm. Fourier-transform infrared (FTIR) spectra of the nanocomposite-CAP nanoparticles and free CAP were obtained using a (Protege 460) FTIR spectrometer (Nicolet, USA). For the FTIR spectroscopy investigations, 10 mg of sample were mixed with 100 mg of KBr and pressed into a pellet. The measurements were carried out in the mid-infrared range of 4000 to 400 cm^{-1} at a resolution of 4 cm^{-1}, with 100 scans recorded and averaged per spectrum. The surface morphologies of the free CAP and nanocomposite-CAP nanoparticles were studied by scanning electron microscopy (SEM, PHENOM PRO X, Netherlands) for which all samples were

coated with a thin film of gold under vacuum before microscopic analysis and then viewed under an accelerating voltage of 10 kV at an appropriate magnification. The hydrodynamic diameter of the nano PMs was measured by dynamic light scattering using a Horiba SZ100 instrument. The CMC was measured using the surface tension method and a Kruss K10 ST tensiometer.

2.3. Preparation of CAP-loaded nano PMs

A co-evaporation method was carried out, in which specific amounts of CD and copolymer were dissolved in distilled water and a specific amount of CAP was dissolved in methanol separately, which was then added dropwise to the CD solution. The solution mixture was then stirred at 52 °C at 100 rpm for 7 h, after which the clear solution was placed in an oven at 50 °C for solvent evaporation to occur and was then heated at 40 °C for 24 h to dry completely.[52]

2.4. Experimental design

The DSD proposed by Jones and Nachtsheim[48] was adopted to investigate the effects of four continuous factors ($k = 4$) for CAP-loaded nano polymeric micelles that were identified, in preliminary runs, as potentially important for the drug loading process, which were the amount of copolymer, temperature, time and copolymer/cyclodextrin ratio. For each factor, natural values corresponding to the coded levels of −1, 0 and 1 were selected to cover a range of values of practical interest based on the results of preliminary experiments conducted to assess their individual effect on the entrapment efficiency. Overall, the experimental design consisted of 13 runs. Of course, it is worth mentioning that there 13 runs were carried out for four factors, which were conducted randomly to minimize the effects of uncontrolled factors. The design, layout and observed entrapment efficiency are shown in Table 1. The design and analysis of experiments were performed using the statistical software Design Expert V11.

2.5. Determination of drug con0074ent and entrapment efficiency

The drug content of the CAP-loaded nano PMs was determined by dissolving the formulation in methanol as the nano PMs do not dissolve in methanol and only the CAP medicine that is not entrapped dissolves in methanol. This was then centrifuged and the concentration of free drug in the supernatant was measured using a UV-vis spectrophotometer at a wavelength of 240 nm, resulting in the amount of drug being absorbed according to eqn (1) and (2).

$$C_e = C_i - C_s \quad (1)$$

$$\mathrm{EE(entrapment\ efficiency)} = \frac{C_e}{C_i} \times 100 \quad (2)$$

where C_e is the amount of drug trapped (encapsulated); C_i is the initial drug value; C_s is the drug value in the supernatant; and EE is the drug entrapment efficiency.

2.6. *In vitro* drug release

The release of CAP from nano PMs was studied using pH-sensitive drug delivery systems employing a dialysis bag in solutions with different pH values. A certain amount of CAP-loaded nano PM solution was introduced into the dialysis bag (cellulose membrane, molecular weight cut off of 12 400 Da). The bag was hermetically sealed and immersed in 50 mL of 0.1 N hydrochloric acid. The entire arrangement was maintained at 37 ± 0.5 °C with continuous magnetic stirring at 50 rpm for 2 h. After 2 h, the dissolution medium was replaced with 50 mL of pH 4.5 acetate buffer and the study was extended for a further 2 h. Uninterruptedly, dissolution was continued in pH 7.4 phosphate buffer for 24 h. At a selected time interval, samples were removed and replaced with fresh medium to maintain sink conditions. The samples were analyzed using a UV spectrophotometer to determine the CAP content.[52–60] The cumulative release amount of drug (E_n) was calculated according to eqn (3), and the cumulative rate of drug release was calculated according to eqn (4):

Table 1 Experimental design layouts and observed response (y)

Run	X_1 (amount of copolymer), mg	X_2 (temperature), °C	X_3 (time), h	X_4 (CP/CD), ratio	Y (entrapment efficiency)%
1	400	40	1	5	63.50
2	300	40	5	3	71.75
3	200	20	9	3	51.50
4	400	60	1	3	65.00
5	200	60	5	5	68.25
6	400	20	5	1	56.50
7	200	60	1	1	51.25
8	300	20	1	1	39.75
9	200	40	9	1	62.00
10	200	20	1	5	39.25
11	400	20	9	5	60.75
12	300	60	9	5	73.00
13	400	60	9	1	72.75

$$E_n = V_1(C_1 + C_2 + \ldots + C_{n-1}) + V_0C_n \quad (3)$$

$$\text{Cumulative release}(\%) = \frac{E_n}{m_t} \times 100 \quad (4)$$

where V_1 is the volume of the drug-delivery medium, C_n is the concentration of the drug in the drug-delivery medium at the n-th replacement, V_0 is the volume of the initial drug-delivery medium, and m_t is the total drug amount.

3. Results and discussion

3.1. Characterization

Anti-cancer drug capecitabine is soluble in various solvents; however, due to the high solubility in methanol and the use of this solvent in the drug loading step, the spectrophotometry (UV-vis) spectrum of the drug in Fig. 1 was taken in methanol. This has two peaks at 240 and 303 nm. The rest of the materials used in the UV-vis region were not adsorbed.[61]

The FTIR spectrum of CD in Fig. 2 shows characteristic peaks at 3400 and 2854 cm^{-1} due to O–H and C–H stretching vibrations. In addition, peaks at 1650, 1153, 1029, and 841 cm^{-1} can be observed that correspond to HOH, C–O, C–O–C glucose units and the C–O–C of rings of CD, respectively.[62–65]

In the FTIR spectrum of MA–AA copolymer, the peaks at 1721, 1408 and 2890 cm^{-1} represent the C=O stretching vibration, a band for the combination of C–O stretching and O–H in plane deformation vibration, and aliphatic C–H stretching vibration, respectively. The peak at 1639 cm^{-1} in the spectrum of the MA–AA copolymer represents C–C stretching vibration. These data suggest the formation of the copolymer.[66,67] In the FTIR spectrum of the CD + CP composition, the peak at 1639 cm^{-1} represents a C–O stretching vibration, the vibration of C–O–C can be observed at 1153 cm^{-1}, and the peak at 1408 cm^{-1} can be attributed to a combination of C–O stretching and O–H in-plane deformation vibration. The peaks at 1721 and 1639 cm^{-1} can be attributed to the C=O vibration of COOH and the stretching vibration of C–C, respectively,

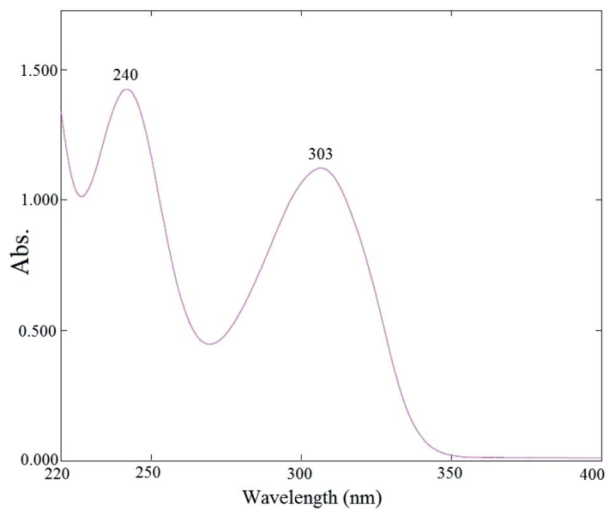

Fig. 1 UV-vis spectrum of CAP in methanol.

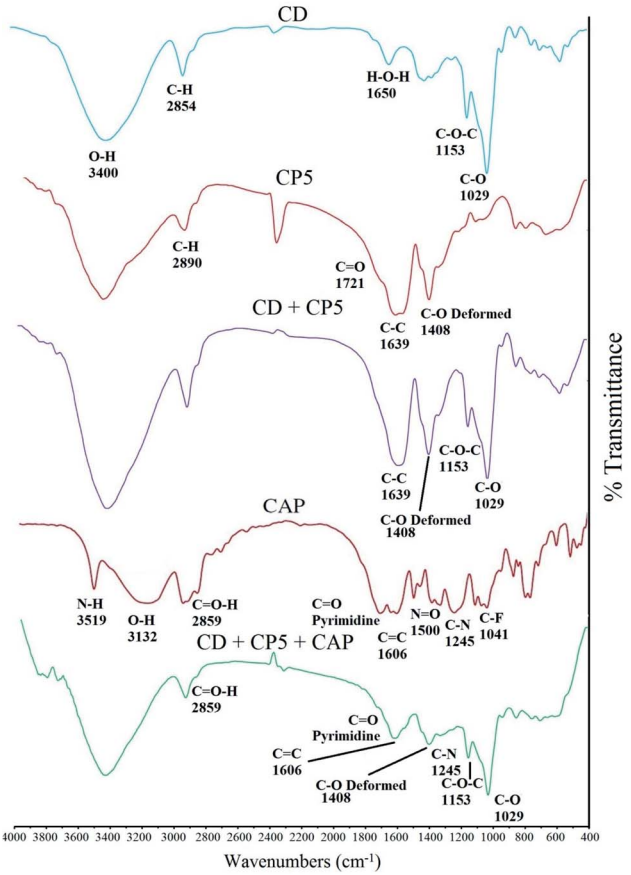

Fig. 2 FTIR spectra of βCD, copolymer, CD + Copolymer, CAP and CD + Copolymer + CAP complex. Measurements performed as KBr disks.

which represent the link between CP5 and CD. For CAP the absorption band appeared were 3519 cm^{-1} and 3132 cm^{-1} (O–H stretching and N–H stretching respectively), at 2968 cm^{-1} shows the C–H stretching, at wave number 2859 cm^{-1} shows the presence of aldehyde group (CH=O), at 1688.90 cm^{-1} (pyrimidine carbonyl stretching vibration), at 1606 cm^{-1} C=C stretching, at 1500 cm^{-1} shows the N=O bending vibrations and further at 1245 cm^{-1} shows the C–N bending vibrations, at 1041.60 cm^{-1} and 1206.49 cm^{-1} (C–F stretching and tetrahydrofuran ring respectively).[68,69] In the spectrum of the combination of CD + CP + CAP, the peaks at 1153 and 1029 cm^{-1} correspond to the C–O and C–O–C glucose units of CD, the peak at 1245 cm^{-1} is related to C–N bending vibrations, that at 1688.90 cm^{-1} to pyrimidine carbonyl stretching vibrations, that at 1606 cm^{-1} to the C=C stretching of CAP, the peak at 1408 cm^{-1} is due to a combination of C–O stretching and the O–H in-plane deformation vibration of CP, where the index peaks of each component are clearly visible.

3.2. Surface morphology analysis

Morphology studies were performed on samples using a SEM (PHENOM PRO X). Fig. 3(a and b) shows that part a is the drug CAP and b shows spherical balls of the drug loaded in the nano

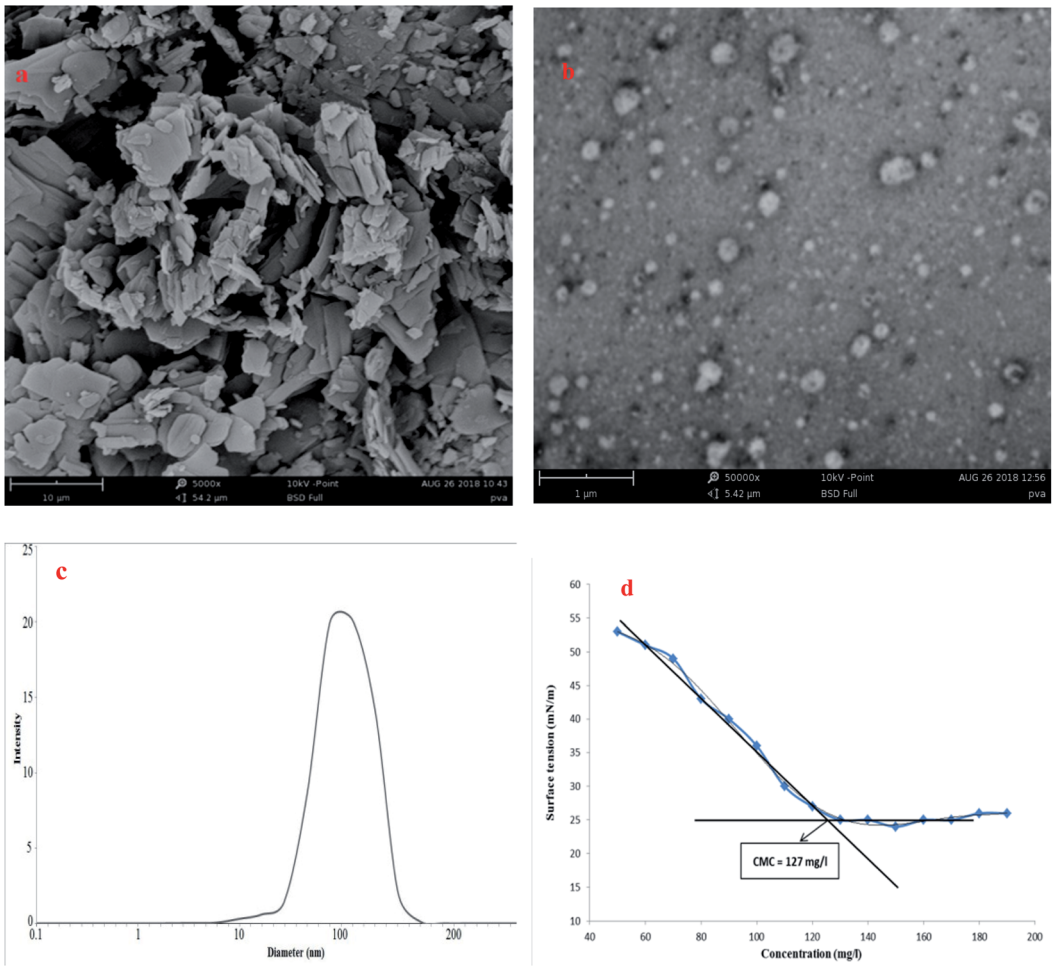

Fig. 3 SEM images of (a) CAP and (b) CAP-loaded nano PMs, and (c) the particle size of nano PMs measured by DLS and (d) determination of the CMC using a surface tension method.

PMs. The hydrodynamic diameter of the suspended nanoparticles was measured by dynamic light scattering, as shown in Fig. 3(c). The CMC value was 127 mg L^{-1}, as shown in Fig. 3(d). These results indicate uniform spherical shapes of the material with diameters of around 50–150 nm.

3.3. Drug entrapment efficiency (EE)

After loading the drug inside the nano PMs and drying them inside an oven, as the nano PMs are not dissolvable in methanol but the drug can be completely dissolved in methanol, 20 mL of methanol was added to the nano PMs and the mixture was stirred for 5 min. The mixture was then centrifuged at 4500 rpm for 10 min, after which the supernatant was separated and its UV-vis spectrum was measured at 240 nm.

3.4. Evaluation of significant variables by DSD

Analysis of DSD data was carried out *via* a two-step procedure involving a stepwise regression. We could be obtained by using the stepwise selection procedure with a *p*-value to enter terms in the model of 0.05, the results of which are presented in Table 2.

3.5. Optimization of effective factors in drug loading

Here, we examine the factors together, starting with the amount of copolymer and temperature factors. As shown in Fig. 4(a), with an increase in the amount of copolymer, there is an increase in entrapment efficiency. One of the factors that greatly affect the percentage of drug loading is the temperature associated with the drug loading step, which was 20–60 °C. According to the results, upon increasing the temperature up to 52 °C, the percentage of drug entrapment efficiency increased and then decreased, probably due to the degradation effect that temperature has on the micelles. Another parameter that has a great effect on the percentage of drug loading is the reaction

Table 2 Estimates of the regression coefficients of the model

Term	Coeff.	*p*-Value
Intercept	71.75	—
A-CP	4.63	0.0343
B-temperature	8.25	0.0148
C-time	6.13	0.0232
D-CP/CD	2.25	0.0024

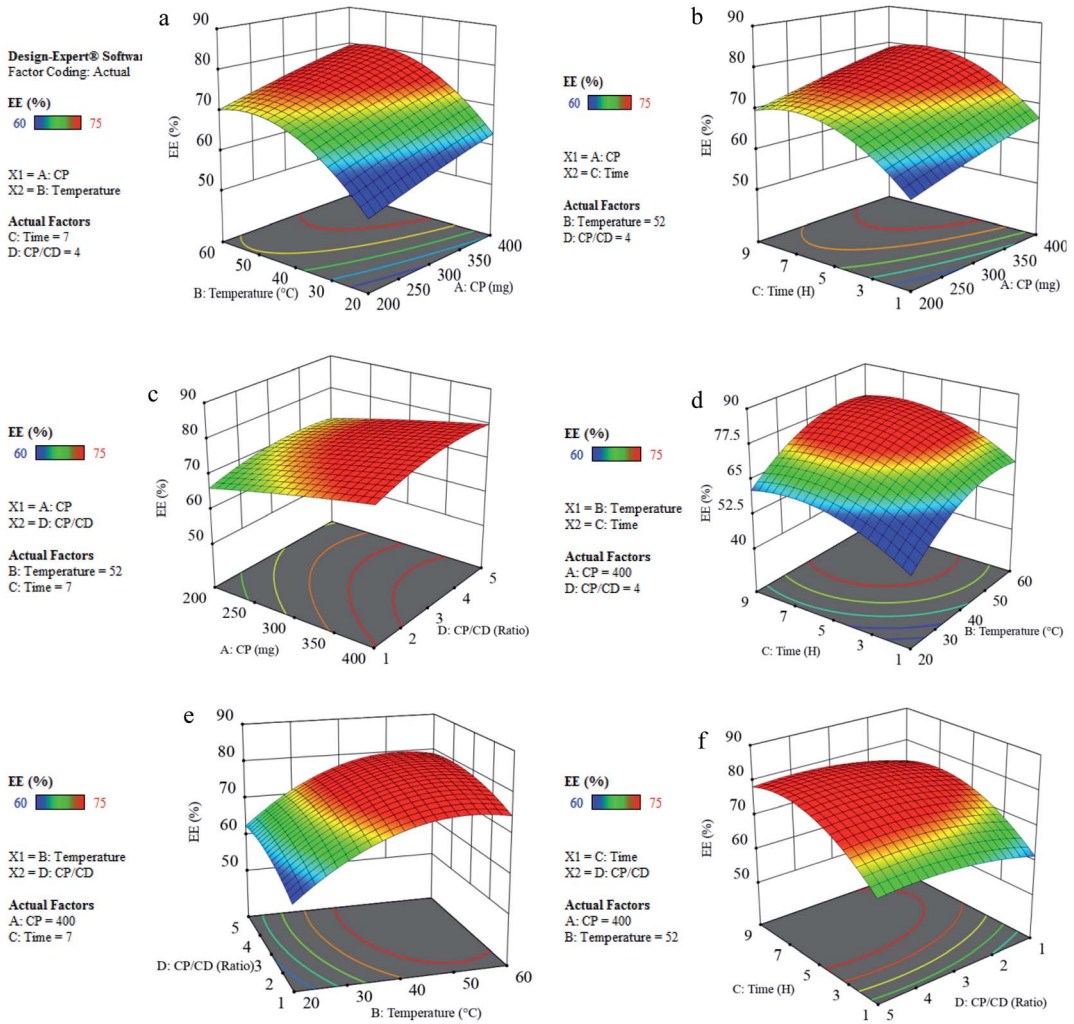

Fig. 4 Showing the simultaneous effects and 3D surface and contour plots of *R* (%) response for drug entrapment efficiency by nano PMs.

time and drug mixing with the nano PMs. The reaction time was a period of 1 to 9 h, after which the percentage of drug entrapment efficiency was measured. As shown in Fig. 4(b), the loading rate increased with increasing reaction time until maximum loading of the drug was achieved after 7 h of reaction. Another item that was examined was the weight ratio of copolymer to cyclodextrin, which was evaluated in ratios of 1 to 5, and the percentage of entrapment efficiency was measured. As indicated in Fig. 4(c), the highest percentage of drug loading is obtained in the ratio 4 copolymer to cyclodextrin, which is probably related to the formation of micelle. The interactions of the parameters can be seen in Fig. 4(d–f). In optimal conditions, the drug loading amount was 80.50%. According to the results obtained in optimal conditions (Table 3), and the standard deviation value, it was determined that the design of the experiment performed with the practical test was in line with the predicted range.

Table 3 Results of the repeatability of the testing and compliance with the design of the experiments

Experiment	Entrapment efficiency%	Average	SD	Acceptable range	Theory
1	80.88	79.68	1.07	78.61–80.75	80.55
2	79.35				
3	78.81				

3.6. Comparison of the drug entrapment efficiency

For this purpose, the percentage of drug loading was tested under several different sets of conditions, the results of which are shown in Fig. 5. In the first stage, only CD was used in the method described for drug loading, in which the percentage capture was 27%. In the second stage, drug loading was achieved with hydroxypropyl-β-cyclodextrin (HPβCD), which gave a value of 32%. In the third stage, the drug was tested with copolymer alone, with a percentage drug loading of 18%. And then with HPβCD and copolymer, which gave a value of 58%. In the final stage of drug loading with CD and copolymer, a value of 80.5% was obtained. Given that the percentage of drug loading with HPβCD was greater than that of CD, it was

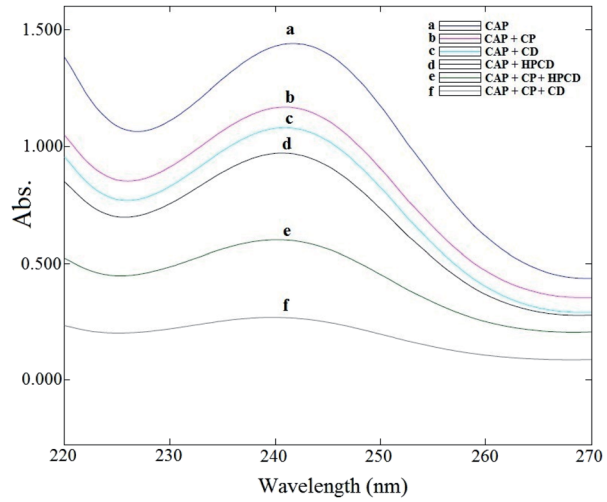

Fig. 5 Comparison of the spectra showing the drug loading of the different compounds.

expected that coagulation in HPβCD with copolymer would be greater than CD with the copolymer. If this is the opposite, it has a lower percentage of drug loading, which is probably due to the higher solubility of HPβCD than the CD, which makes the conditions for the creation of the micelle softer and less drug in the micelle be imprisoned.

3.7. *In vitro* drug release

The release of CAP was carried out for 2 h in an acidic solution of HCl 0.1 M and then 2 h in acetate buffer solution, before being placed in alkaline phosphate buffer in a dialysis bag at 37 °C. As shown in Fig. 6(a), the amount of CAP release during the first two hours, which is in the acidic medium (pH = 1.2), is less than 4%, of which about 2% is at the very first moment, probably due to unloaded drugs and residues at the compound level. It can be said that the percentage of release in this environment is around 2%, as the polymer component of the synthesized compound in the acidic environment forms a closed loop that preserves the drug and does not allow its release. In the next stage, in the acetate buffer, the percentage of drug release reaches about 18%, of which 4% is related to the acidic medium before, and about 14% is related to the acetate buffer medium, which is also formed is stable. Therefore, the percentage of drug release is slow and low.

But after these 4 hours, release occurs in a phosphate buffer and pH 7.4 is similar to that of the colon, as shown in Fig. 6(b), release in this environment is performed at a faster and more controlled speed. This is because the formed micelles are

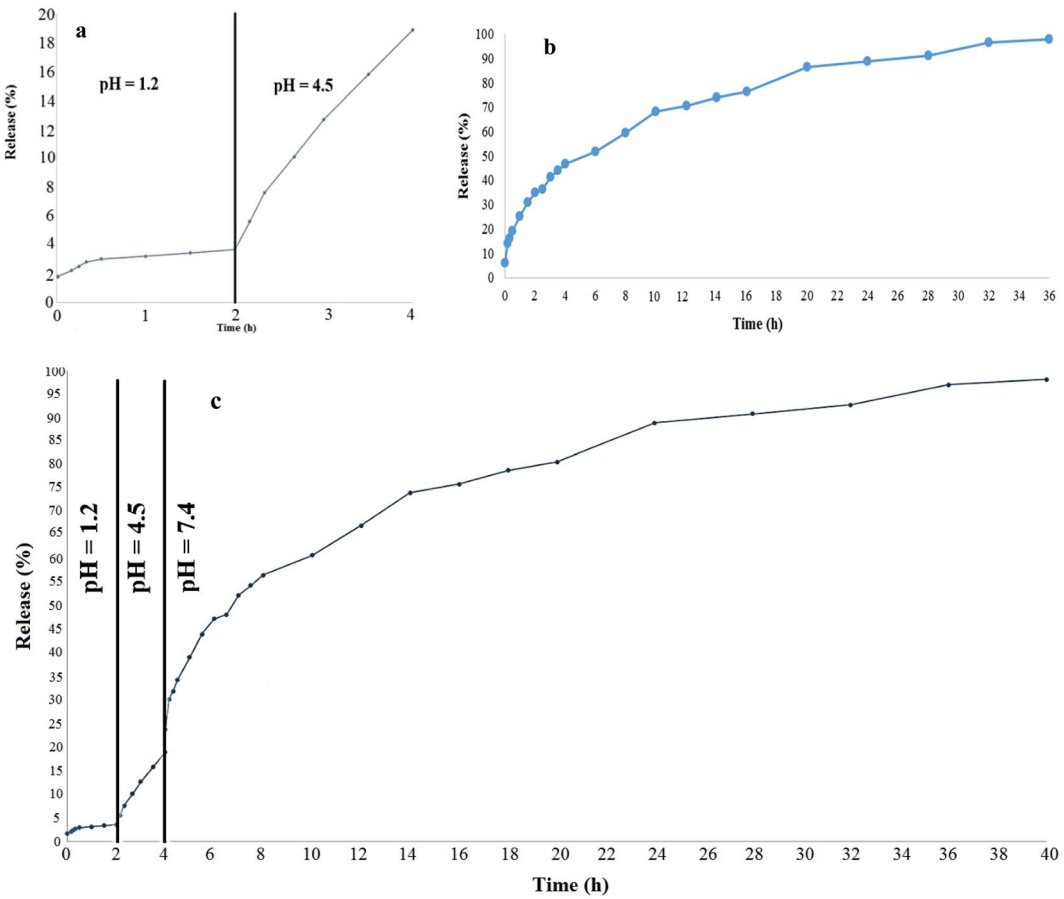

Fig. 6 Release of CAP in (a) an acidic environment, (b) an alkaline environment and (c) from pH 1.2 to pH 7.4.

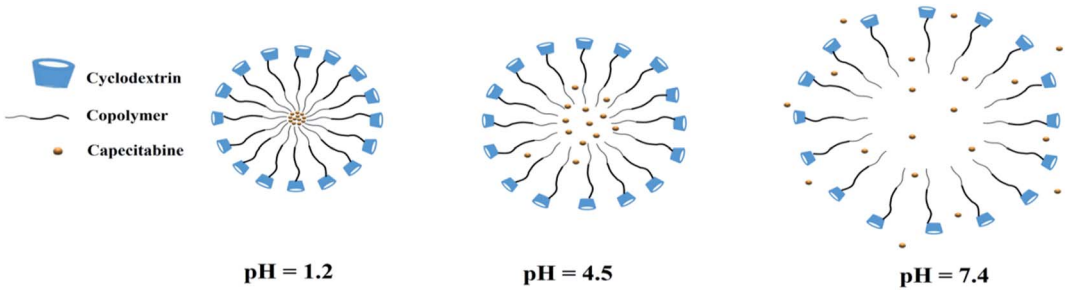

Fig. 7 Mechanism of CAP drug release from the micelles.

opened in this environment and the drug is released in a controlled manner. As can be seen from Fig. 6(c), after around 40 h, 97% of the drug is released, which indicates the high efficiency of the synthesized composition in the controlled transfer of CAP to reach the colon environment. It is worth mentioning that UV-vis spectrophotometry was used to measure the release of the drug. For each environment, a separate calibration curve was drawn along with the release conditions, and the percentage of release according to the calibration curve was obtained in the same environment.

3.8. Drug release mechanism

In Fig. 7, the mechanism of the drug release is that the micelles are formed by a surface layer of CD, with the internal layer comprising copolymer and drug. At pH 1.2, the micelles are completely closed and do not allow the release of drugs. At pH 4.5, the micelles open slightly and some of the drug is released, but there is not much freedom of action given to the drug. Finally, at 7.4 pH, the micelles begin to fully open and the drug is released in a controlled manner. Thus, the pH of the surrounding medium relative to respective pK_a and pK_b values of the pendant groups is related to the swelling of polyacids with acidic or basic pendant groups. For an anionic matrix (with –COOH groups), if the medium pH is more than the pK_a of the acidic groups of the polymers, ionization of the acidic groups of the polymer matrix occurs, resulting in the formation of set negative charges ($-COO^-$) on the polymer backbone, with the positive charges (H^+) mobile in the fluid medium. Hence, there exists an electrostatic repulsion between the polymer chains, leading to the swelling of the matrix and at the same time de-swelling occurs if the pH is less than the pK_a.[70] The drug-release behaviour of nano PMs micelles with different pH values is shown in Fig. 7. In terms of nano PMs micelles, the release of CAP at pH 1.2 within 2 h accounts for only 4%, indicating that the drug is well-protected in the simulated gastric fluid. At pH 7.4, 70.4% CAP was released within 12 h and 97% was released within 36 h, where the release of CAP was significantly hastened under simulated colon conditions. Fig. 7 illustrates the drug-release mechanism at different pH values. The nano PMs chains curl up in the acidic environment and may tightly wrap around the hydrophobic core, making it difficult for the CAP to be released. In a neutral environment, the carboxyl groups are gradually deprotonated and the nano PMs chains relax, hence, the CAP can be steadily released. Considering the environmental changes in the human body, a small amount of the drug can be released in the stomach, and when the nano PMs micelles reach the colon, the drug is released continuously. This release pattern of the nano PMs micelles is in accordance with the requirements for oral administration of a drug.[71]

4. Conclusion

We synthesized amphiphilic copolymer PMs, which could be induced to self-assemble into spherical nanomicelles. The results showed that the combination of CD with acrylic maleic copolymer exhibits a much better performance than the single components alone in terms of drug loading. A novel design of experiments (DOE) approach was successfully employed to understand and optimize the formulation and process parameters for the preparation of the nano PMs, ensuring quality assurance in the product development process. It was found that a simple and inexpensive method could be used to formulate anticancer drugs that could be better controlled and targeted to release the drug to reduce complications and make them more effective. One of the major uses of CAP drug therapy is in colon cancer. In this research, we tried to develop nano PMs that have a low release rate before entering the intestines to aim for maximum drug release in the colon environment. The results show that the nano PMs meet this requirement well, with over 80% of the drug being released into the colon environment. The present study proves that nano PMs could be a promising and potential material for the formulation of anticancer drugs such as CAP to provide effective treatment for colon cancer.

Conflicts of interest

The authors declare that they have no known competing financial interests or personal relationships that could have appeared to influence the work reported in this paper.

Acknowledgements

We acknowledge financial support from the University of Guilan (Rasht, Iran).

References

1 Y. Meissner and A. Lamprecht, Alternative Drug Delivery Approaches for the Therapy of Inflammatory Bowel Disease, *J. Pharm. Sci.*, 2008, **97**, 2878–2891.
2 A. Lamprecht, H. Yamamoto, H. Takeuchi and Y. Kawashima, Microsphere design for the colonic delivery of 5-fluorouracil, *J. Controlled Release*, 2003, **90**, 313–322.
3 R. C. Mundargi, S. A. Patil, S. A. Agnihotri and T. M. Aminabhavi, Development of Polysaccharide-Based Colon Targeted Drug Delivery Systems for the Treatment of Amoebiasis, *Drug Dev. Ind. Pharm.*, 2007, **33**, 255–264.
4 J. A. Fix, Oral controlled release technology for peptides: status and future prospects, *Pharm. Res.*, 1996, **13**, 1760–1764.
5 P. Langguth, V. Bohner, J. Heizmann, H. P. Merkle, S. Wolffram, G. L. Amidon and S. Yamashita, The challenge of proteolytic enzymes in intestinal peptide delivery, *J. Controlled Release*, 1997, **46**, 39–57.
6 M. Mackay, J. Phillips and J. Hastewell, Peptide drug delivery: Colonic and rectal absorption, *Adv. Drug Delivery Rev.*, 1997, **28**, 253–273.
7 M. Katsuma, S. Watanabe, H. Kawai, S. Takemura and K. Sako, Effects of absorption promoters on insulin absorption through colon-targeted delivery, *Int. J. Pharm.*, 2006, **307**, 156–162.
8 L. Yang, Biorelevant dissolution testing of colon-specific delivery systems activated by colonic microflora, *J. Controlled Release*, 2008, **125**, 77–86.
9 B. J. Rider, *Capecitabine, xPharm: The Comprehensive Pharmacology Reference*, 2007, pp. 1–4.
10 K. K. H. Goey, S. G. Elias and H. van Tinteren, Maintenance treatment with capecitabine and bevacizumab versus observation in metastatic colorectal cancer: updated results and molecular subgroup analyses of the phase 3 CAIRO3 study, *Ann. Oncol.*, 2017, **28**, 2128–2134.
11 A. Polk, M. Vaage-Nilsen, K. Vistisen and D. L. Nielsen, Cardiotoxicity in cancer patients treated with 5-fluorouracil or capecitabine: a systematic review of incidence, manifestations and predisposing factors, *Cancer Treat. Rev.*, 2013, **39**(8), 974–984.
12 M. Upadhyay, S. K. R. Adena, H. Vardhan, S. Pandey and B. Mishra, Development and optimization of locust bean gum and sodium alginate interpenetrating polymeric network of capecitabine, *Drug Dev. Ind. Pharm.*, 2018, **44**(3), 511–521.
13 M. Upadhyay and S. K. R. Adena, Development of biopolymers based interpenetrating polymeric network of capecitabine: A drug delivery vehicle to extend the release of the model drug, *Int. J. Biol. Macromol.*, 2018, **115**, 907–919.
14 B. Reigner, K. Blesch and E. Weidekamm, Clinical pharmacokinetics of capecitabine, *Clin. Pharmacokinet.*, 2001, **40**(2), 85–104.
15 C. Kelly, N. Bhuva, M. Harrison, A. Buckley and M. Saunders, Use of raltitrexed as an alternative to 5-fluorouracil and capecitabine in cancer patients with cardiac history, *Eur. J. Cancer*, 2013, **49**(10), 2303–2310.
16 R. Midgley and D. J. Kerr, Capecitabine: have we got the dose right?, *Nat. Clin. Pract. Oncol.*, 2009, **6**(1), 17–24.
17 E. M. Martin, Cyclodextrins and their uses: a review, *Process Biochem.*, 2004, **39**, 1033–1046.
18 A. Hedges, *Chapter 22 - Cyclodextrins: Properties and Applications, Starch*, Chemistry and Technology Food Science and Technology, 3rd edn, 2009, pp. 833–851.
19 T. Loftsson and D. Duchêne, Cyclodextrins and their pharmaceutical applications, *Int. J. Pharm.*, 2007, **329**, 1–11.
20 B. Flourié, C. Molis, L. Achour, H. Dupas, C. Hatat and J. C. Rambaud, Fate of β-Cyclodextrin in the Human Intestine, *J. Nutr.*, 1993, **123**, 676–680.
21 V. R. Sinha and R. Kumria, Polysaccharides in colon-specific drug delivery, *Int. J. Pharm.*, 2001, **224**, 19–38.
22 M. K. Chourasia and S. K. Jain, Pharmaceutical approaches to colon targeted drug delivery systems, *J. Pharm. Pharm. Sci.*, 2003, **6**, 33–66.
23 C. Giardina and M. S. Inan, Nonsteroidal anti-inflammatory drugs, short-chain fatty acids, and reactive oxygen metabolism in human colorectal cancer cells, *Biochim. Biophys. Acta*, 1998, **1401**, 277–288.
24 D. T. Pham and A. Chokamonsirikun, Polymeric micelles for pulmonary drug delivery: a comprehensive review, *J. Mater. Sci.*, 2021, **56**, 2016–2036.
25 L. Qiu and M. Zhu, pH-triggered degradable polymeric micelles for targeted anti-tumor drug delivery, *Mater. Sci. Eng., C*, 2017, **78**, 912–922.
26 T. A. B. Kuchekar and A. P. Pawar, *Int. Conf. Adv. Nanomater. Emerging Eng. Technol.*, 2013, **2013**, 412–415.
27 Y. Wang and J. van. Steenbergen, Biotin-decorated all-HPMA polymeric micelles for paclitaxel delivery, *J. Controlled Release*, 2020, **328**, 970–984.
28 T. Chen and L. Tu, Multi-functional chitosan polymeric micelles as oral paclitaxel delivery systems for enhanced bioavailability and anti-tumor efficacy, *Int. J. Pharm.*, 2020, **578**, 119105.
29 L. P. Sze and H. Y. Li, Oral delivery of paclitaxel by polymeric micelles: A comparison of different block length on uptake, permeability and oral bioavailability, *Colloids Surf., B*, 2019, **184**, 110554.
30 S. Karimi and H. Namazi, Synthesis of folic acid-conjugated glycodendrimer with magnetic β-cyclodextrin core as a pH-responsive system for tumor-targeted co-delivery of doxorubicin and curcumin, *Colloids Surf., A*, 2021, **627**, 127205.
31 K. Ramesh and C. K. Balavigneswaran, Synthesis of cyclodextrin-derived star poly(N-vinylpyrrolidone)/poly(lactic-co-glycolide) supramolecular micelles via host-guest interaction for delivery of doxorubicin, *Polymer*, 2021, **214**, 123243.
32 M. Y. Wang and Y. Qu, Methotrexate-loaded biodegradable polymeric micelles for lymphoma therapy, *Int. J. Pharm.*, 2019, **557**, 74–85.
33 S. J. Moon and D. G. You, pH-Sensitive Polymeric Micelles as the Methotrexate Carrier for Targeting Rheumatoid Arthritis, *Macromol. Res.*, 2020, **28**, 99–102.

34 G. S. Kwon and K. Kataoka, Block copolymer micelles as long-circulating drug vehicles, *Adv. Drug Delivery Rev.*, 2012, **64**, 237–245.
35 Z. Ahmad, Polymeric micelles as drug delivery vehicles, *RSC Adv.*, 2014, **4**(33), 17028–17038.
36 U. Kedar, Advances in polymeric micelles for drug delivery and tumor targeting, *Nanomedicine*, 2010, **6**(6), 714–729.
37 H. Cabral and K. Kataoka, Progress of drug-loaded polymeric micelles into clinical studies, *J. Controlled Release*, 2014, **190**, 465–476.
38 A. E. Felber and M. H. Dufresne, pH-sensitive vesicles, polymeric micelles, and nanospheres prepared with polycarboxylates, *Adv. Drug Delivery Rev.*, 2012, **64**(11), 979–992.
39 S. Kim, Hydrotropic polymer micelles containing acrylic acid moieties for oral delivery of paclitaxel, *J. Controlled Release*, 2008, **132**(3), 222–229.
40 V. P. Sant and D. Smith, Novel pH-sensitive supramolecular assemblies for oral delivery of poorly water soluble drugs: preparation and characterization, *J. Controlled Release*, 2004, **97**(2), 301–312.
41 V. P. Sant and D. Smith, Enhancement of oral bioavailability of poorly water-soluble drugs by poly (ethylene glycol)-block-poly (alkyl acrylate-co-methacrylic acid) self-assemblies, *J. Controlled Release*, 2005, **104**(2), 289–300.
42 G. Gaucher, Polymeric micelles for oral drug delivery, *Eur. J. Pharm. Biopharm.*, 2010, **76**(2), 147–158.
43 M. Ghezzi and S. Pescina, Polymeric micelles in drug delivery: An insight of the techniques for their characterization and assessment in biorelevant conditions, *J. Controlled Release*, 2021, **332**, 312–336.
44 J. S. Choi and N. H. Cho, Comparison of paclitaxel solid dispersion and polymeric micelles for improved oral bioavailability and in vitro anti-cancer effects, *Mater. Sci. Eng., C*, 2019, **100**, 247–259.
45 X. Wang, Preparation and evaluation of carboxymethyl chitosan-rhein polymeric micelles with synergistic antitumor effect for oral delivery of paclitaxel, *Carbohydr. Polym.*, 2019, **206**, 121–131.
46 R. Kumar and A. Sirvi, Polymeric micelles based on amphiphilic oleic acid modified carboxymethyl chitosan for oral drug delivery of bcs class iv compound: Intestinal permeability and pharmacokinetic evaluation, *Eur. J. Pharm. Sci.*, 2020, **153**, 105466.
47 W. Y. Hu and Z. M. Wu, Smart pH-responsive polymeric micelles for programmed oral delivery of insulin, *Colloids Surf., B*, 2019, **183**, 110443.
48 J. B. Nachtsheim, A class of Three-Level Designs for Definitive Screening in the Presence of Second-Order Effects, *Journal of Quality Technology*, 2011, **43**, 1–15.
49 M. Saha and D. R. Saha, QbD based development of resveratrol-loaded mucoadhesive lecithin/chitosan nanoparticles for prolonged ocular drug delivery, *J. Drug Delivery Sci. Technol.*, 2021, **63**, 10248.
50 R. Sh. Gabbay and R. S. Kenett, Synchronizing the release rates of salicylate and indomethacin from degradable chitosan hydrogel and its optimization by definitive screening design, *Eur. J. Pharm. Sci.*, 2018, **125**, 102–109.
51 J. M. Goldman and H. T. More, Optimization of Primary Drying in Lyophilization During Early-Phase Drug Development Using a Definitive Screening Design With Formulation and Process Factors, *J. Pharm. Sci.*, 2018, **107**, 2592–2600.
52 L. Zhang and Q. Zhang, Drug-in-cyclodextrin-in-liposomes: A novel drug delivery system for flurbiprofen, *Int. J. Pharm.*, 2015, **492**, 40–45.
53 L. Cheng and B. Deng, pH-Responsive Lignin-Based Nanomicelles for Oral Drug Delivery, *J. Agric. Food Chem.*, 2020, **68**, 5249–5258.
54 P. Sinha and U. Udhumansha, Capecitabine encapsulated chitosan succinate-sodium alginate macromolecular complex beads for colon cancer targeted delivery: in vitro evaluation, *Int. J. Biol. Macromol.*, 2018, **117**, 840–850.
55 A. Patel and N. Bhatt, Colon Targeted Drug Delivery System, *Journal of Pharmaceutical Science and Bioscientific Research*, 2011, **1**, 37–49.
56 W. Gao and J. M. Chan, pH-Responsive Nanoparticles for Drug Delivery, *Mol. Pharm.*, 2010, **7**, 1913–1920.
57 J. Liu and Y. Huang, pH-Sensitive nano-systems for drug delivery in cancer therapy, *Biotechnol. Adv.*, 2014, **32**, 693–710.
58 Z. Wang and X. Deng, Mechanisms of drug release in pH-sensitive micelles for tumor targeted drug delivery system, *Int. J. Pharm.*, 2017, **535**, 1–34.
59 A. Gandhi and S. Jana, In-vitro release of acyclovir loaded Eudragit RLPO® nanoparticles for sustained drug delivery, *Int. J. Biol. Macromol.*, 2014, **67**, 478–482.
60 L. F. A. Asghar and S. Chandran, Design and evaluation of pH modulated controlled release matrix systems for colon specific delivery of indomethacin, *Pharmazie*, 2008, **63**, 736–742.
61 G. Ramesh and M. S. Rao, Development and Validation of A Simple and Specific UV Spectrophotometric Method for Capecitabine Assay in Active Pharmaceutical Ingredients (API) and in its Dosage Forms, *Int. J. Pharm. Pharm. Res.*, 2015, **2**, 152–160.
62 M. M. Yallapu and M. Jaggi, β-Cyclodextrin-curcumin self-assembly enhances curcumin delivery in prostate cancer cells, *Colloids Surf., B*, 2010, **79**, 113–125.
63 K. P. Sambasevam and S. Mohamad, Synthesis and Characterization of the Inclusion Complex of β-cyclodextrin and Azomethine, *Int. J. Mol. Sci.*, 2013, **14**, 3671–3682.
64 K. Sivakumar and G. Parinamachivayam, Preparation, characterization and molecular modeling studies of the beta-cyclodextrin inclusion complex with benzoguanamine and its analytical application as chemosensor for the selective sensing of Ce^{4+}, *Spectrochim. Acta, Part A*, 2018, **200**, 212–225.
65 A. Moreira and V. Bittencourt, Hydrophobic nanoprecipitates of β cyclodextrin/avermectins inclusion compounds reveal insecticide activity against Aedes aegypti

larvae and low toxicity against fibroblasts, *J. Agric. Food Chem.*, 2018, **66**, 7275–7285.

66 B. Senthilmurugan and B. Ghosh, Maleic acid based scale inhibitors for calcium sulfate scale inhibition in high temperature application, *J. Pet. Sci. Eng.*, 2010, **75**, 189–195.

67 B. L. Rivas and G. V. Seguel, Poly (acrylic acid-co-maleic acid)–metal complexes with copper, cobalt, and nickel Synthesis, characterization and structure of its metal chelates, *Polyhedron*, 1999, **18**, 2511–2518.

68 M. Upadhyay and S. Adena, Development of biopolymers based interpenetrating polymeric network of capecitabine: A drug delivery vehicle to extend the release of the model drug, *Int. J. Biol. Macromol.*, 2018, **115**, 907–919.

69 B. Anbarasan and V. A. Niranjana, Development of formulation and in-vitro evaluation of capecitabine loaded Fe_3O_4 nanoparticles modified with PLGA-PEG polymer for colon cancer treatment, *Sri Ramachandra J. Med.*, 2015, **8**, 1–8.

70 B. Anbarasan and S. Rekha, Optimization of the formulation and in-vitro evaluation of capecitabine niosomes for the treatment of colon cancer, *Int. J. Pharm. Sci. Res.*, 2013, **4**, 1504–1513.

71 R. V. Kulkarni, S. Z. Inamdar, *Polysaccharide-based stimuli- 7 sensitive graft copolymers for drug delivery*, 1st edn, 2019, ch. 7, pp. 155–177.